

## Trace Elements and Rare Earth Elements of Sulfide Minerals in the Tianqiao Pb-Zn Ore Deposit, Guizhou Province, China

ZHOU Jiayi<sup>1,2</sup>, HUANG Zhilong<sup>1,\*</sup>, ZHOU Guofu<sup>1</sup>, LI Xiaobiao<sup>1,2</sup>,  
DING Wei<sup>1,2</sup> and BAO Guangping<sup>1,2</sup>

1 State Key Laboratory of Ore Deposits Geochemistry, Institute of Geochemistry, Chinese Academy of Sciences, Guiyang 550002, China

2 Graduate University of Chinese Academy of Sciences, Beijing 100049, China

**Abstract:** Trace elements and rare earth elements (REE) of the sulfide minerals were determined by inductively-coupled plasma mass spectrometry. The results indicate that V, Cu, Sn, Ga, Cd, In, and Se are concentrated in sphalerite, Sb, As, Ge, and Tl are concentrated in galena, and almost all trace elements in pyrite are low. The Ga and Cd contents in the light-yellow sphalerites are higher than that in the brown and the black sphalerites. The contents of Ge, Tl, In, and Se in brown sphalerites are higher than that in light-yellow sphalerites and black sphalerites. It shows that REE concentrations are higher in pyrite than in sphalerite, and galena. In sphalerites, the REE concentration decreases from light-yellow sphalerites, brown sphalerites, to black sphalerites. The ratios of Ga/In are more than 10, and Co/Ni are less than 1 in the studied sphalerites and pyrites, respectively, indicating that the genesis of the Tianqiao Pb–Zn ore deposit might belong to sedimentary-reformed genesis associated with hydrothermal genesis. The relationship between LnGa and LnIn in sphalerite, and between LnBi and LnSb in galena, indicates that the Tianqiao Pb–Zn ore deposit might belong to sedimentary-reformed genesis. Based on the chondrite-normalized REE patterns,  $\delta\text{Eu}$  is a negative anomaly (0.13–0.88), and  $\delta\text{Ce}$  does not show obvious anomaly (0.88–1.31); all the samples have low total REE concentrations (<3 ppm) and a wide range of light rare earth element/high rare earth element ratios (1.12–12.35). These results indicate that the ore-forming fluids occur under a reducing environment. Comparison REE compositions and parameters of sphalerites, galenas, pyrites, ores, altered dolostone rocks, strata carbonates, and the pyrite from Lower Carboniferous Datang Formation showed that the ore-forming fluids might come from polycomponent systems, that is, different chronostratigraphic units could make an important contribution to the ore-forming fluids. Combined with the tectonic setting and previous isotopic geochemistry evidence, we conclude that the ore-deposit genesis is hydrothermal, sedimentary reformed, with multisources characteristics of ore-forming fluids.

**Key words:** trace element, rare earth element, sphalerite, galena, pyrite, deposit genesis, Tianqiao Pb–Zn ore deposit

### 1 Introduction

The Sichuan–Yunnan–Guizhou Pb–Zn metallogenic area (SYG MA) is one of the source bases of Pb, Zn, Ag, and Ge in China. At present, more than 400 Pb–Zn (–Ag) ore deposits and ore spots have been found in this area (Liu and Lin, 1999). Northwest of the Guizhou Pb–Zn metallogenic region (NG MR) is an important part of the SYG MA, with more than 100 ore (spots) deposits (Jin, 2008). The Tianqiao Pb–Zn ore deposit of Guizhou province,

representative of the medium-sized deposits in this area (Fig. 1), is located in the southeast of the SYG MA and in the center of the NG MR. This deposit is characterized by large-scale Pb+Zn reserves (more than 0.2 million tons), high Pb+Zn grades (Pb+Zn contents mostly higher than 20 wt%, parts of ores exceed 30 wt%), and an abundant of associated, useful elements (such as Cd, Ga, and In).

The ore geology (Tang, 1984; Wang, 1994; Mao, 2001; Jin, 2008), ore-controlling structures (Zheng, 1992; Jin, 2008), ore-forming ages (Guan and Li, 1999; Huang et al., 2004; Li, 2004; Jin, 2008), and ore-deposit genesis (Zheng,

\* Corresponding author. E-mail: huangzhilong@vip.gyig.ac.cn

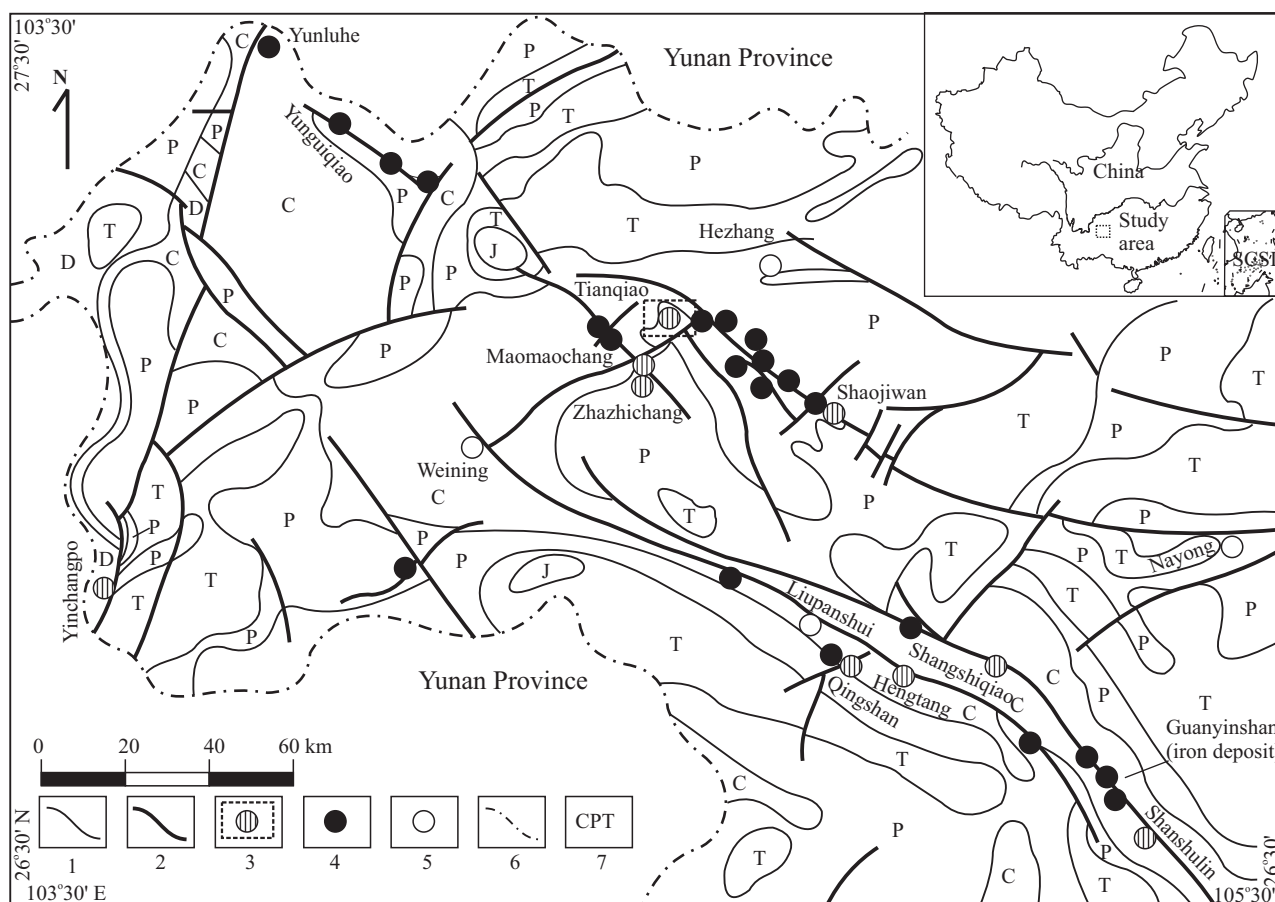


Fig. 1. Aerial geologic sketch map of the northwest Guizhou Pb–Zn metallogenic region (after Liu, 2002).

1. Type-boundary section; 2, faults; 3, medium-sized deposits (including Tianqiao); 4, small-sized deposits; 5, place name; 6, province boundary; 7, strata of Carboniferous, Permian, and Triassic.

1994; Liu and Lin, 1999; Zhou et al., 2001; Huang et al., 2004; Gu, 2006; Jin et al., 2007; Jin, 2008; Zhou et al., 2009) have been previously studied. Tang (1984) and Chen (1986) considered that ore-forming metals/fluids are derived from carbonate hosts, and Zheng (1994) assumed that they are derived from the underlying strata and basement rocks (Zheng, 1994; Mao et al., 1998; Qian, 2001). Liu and Lin (1999) associated their source characters with multisources, that is, the ore host rocks, underlying strata and basement rocks, as well as the Emeishan basalt magmatic activity formed the ore-forming metals/fluids, and the magmatic activity also provided a heat source (Liu and Lin, 1999; Han et al., 2001; Liu et al., 2003; Huang et al., 2004). However, Gu (2006) believed that the Emeishan basalt has no relationship with deposits in this area, except the spatial distribution overlap. Because of the controversy associated with the source of ore-forming metals/fluids of this deposit, the genesis of the deposit is still under debated (Zheng, 1994; Liu and Lin, 1999; Zhou et al., 2001; Huang et al., 2004; Gu, 2006; Jin et al., 2007; Jin, 2008; Zhou et al., 2009).

The trace element compositions of the sulfide minerals

and their ratios (such as the ratios of the Ga/In, Zn/Cd, and Co/Ni) were used to distinguish Pb–Zn ore-deposit types effectively (Hawley and Nichol, 1961; Price, 1972; Liu et al., 1984; Tu et al., 1984; Zhang, 1987; Brill, 1989; Palero-Fernández and Martín-Izard, 2005), and the geochemical behavior of the rare earth elements (REE) showed consistency, making them widely used in tracing ore-forming metals/fluids (Barrett et al., 1990; Bau, 1991; Mills and Elderfield, 1995; Wang et al., 2004; Wilkinson et al., 2005; Huang et al., 2007; Li et al., 2007; Huang et al., 2010). Based on the trace elements and REE compositions of the sulfide minerals from the Tianqiao Pb–Zn deposit, the genesis of the deposit is discussed in the present study.

## 2 Geologic Setting

The Tianqiao Pb–Zn ore deposit is located in the central northwest of Guizhou province and mid-east of the SYG MA, on the southwest margin of the Yangtze Craton (Fig. 1). It is approximately 60 km away from Hezhang County. Geologically, it is situated in the Maomaochang–Shashilang ramp system of the Shuicheng Fault subsidence

(Mao, 2001; Jin, 2008) (Fig. 2). The industrial ore bodies occurred in the dolomitic limestone and dolomite of the Lower Carboniferous Datang Formation ( $C_{1d}$ ) and Baizuo Formation ( $C_{1b}$ ), respectively, which belongs to the northwest-trending, nose-like plunging of the northwest-trending Tianqiao anticline, and is controlled by the  $F_{37}$  fault.

The exposed strata in the ore field from new to old are mainly the Lower Permian Qixia–Maokou Formation and Liangshan Formation ( $P_{1l}$ ), Upper Carboniferous Maping Formation and Huanglong Formation ( $C_{2h}$ ), Lower Carboniferous  $C_{1b}$  and  $C_{1d}$ , Upper Devonian Rongxian Formation ( $D_{3r}$ ), and Middle Devonian Dushan Formation. In addition, the Lower Permian  $P_{1l}$  is not carbonate; the rest are all carbonate rocks, of which the lime–dolomite and dolomite of  $C_{2h}$ ,  $C_{1b}$ ,  $C_{1d}$ , and  $D_{3r}$  are the main ore-bearing rocks.

The main ore bodies of the Tianqiao Pb–Zn ore deposit are produced in the interlayer crushed zone of the  $F_{37}$  fault, which show a stratoid shape, platy ore body, and lenticular form. The boundaries between ore bodies and host rocks are clear, and the occurrence is basically consistent with the stratigraphy (Figs. 2, 3). Thirty-two ore bodies have been found and divided into two sections. The south section is Yingpanshang, which is 400 m in length and 300 m in width, and includes 15 ore bodies. The hosted strata are the  $D_{3r}$ ,  $C_{1b}$ , and  $C_{1d}$ . The larger ore body, which is 200 m in length, 100 m in width, and 1.3–1.8 m in thickness, was produced in the limestone and dolomite of  $C_{1b}$ . The average grade of Pb is 1.23 wt%, and Zn is 5.69 wt%. The Shazidi section, in which the ore-belt length is 800 m and the width is 500 m, is located in the north. There are 17 ore bodies, shaped like the en echelon lenses and sack-like output. The hosted rocks are the dolomite of  $C_{1d}$  and limestone of  $C_{2h}$ , of which III-6 and III-7 are the two largest ore bodies. The III-6 ore body is 250 m in length, 120 m in width, and 1.4–19 m in thickness; the average grade of Pb is 5.51 wt% and Zn is 15 wt%. The III-7 ore body is 320 m in length, 220 m in width, and 1.7–5.15 m in thickness; the average grades of Pb and Zn are 3.6 wt% and 6.52 wt%, respectively. The total reserve amount of the II and III ore bodies is more than 0.2 Mt.

According to microscopic observations and electron-probe microanalysis studies, ores are mainly self-shaped,

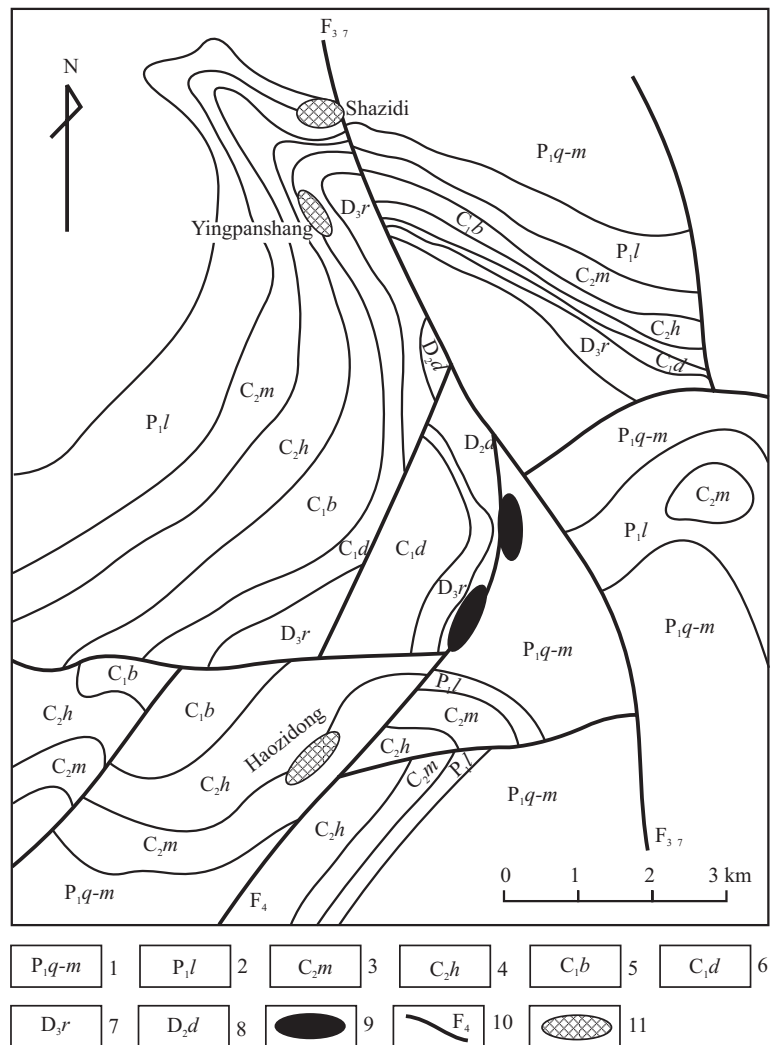


Fig. 2. Geologic sketch map of the Tianqiao ore deposit (after Jin, 2008).

1, Qixia–Maokou Formation; 2, Liangshan Formation; 3, Maping Formation; 4, Huanglong Formation; 5, Baizuo Formation; 6, Datang Formation; 7, Rongxian Formation; 8, Dushan Formation; 9, diabase; 10, abnormal fault; 11, ores.

semiself-shaped, granular, corroded, metasomatic harbor-like, knot-edge, replacement island arc, and metasomatic vein-like in texture. The textures of the oxidized ores are usually granular and string-like. The structures of ores are massive, dip-dyed, and of breccia structure. The structures of oxidized ores are usually earthy, hull-shaped, and grape-like structures. The metal sulfide minerals species include galena, sphalerite, pyrite, chalcopyrite, and a small amount of marcasites. The oxidized minerals species include cerusite, anglesite, siderite, calamine, hemimorphite and hydrozincite. The gangue minerals are mainly calcite and quartz in a small quantity. The wall-rock alterations are mainly dolomitization, pyritization, Fe–Mn carbonation, ferritization, calcitization, and silicification.

According to the ore textures and structures, the vein interpenetration relations and the mineral paragenetic associations (Fig. 4), the ore-forming processes of the

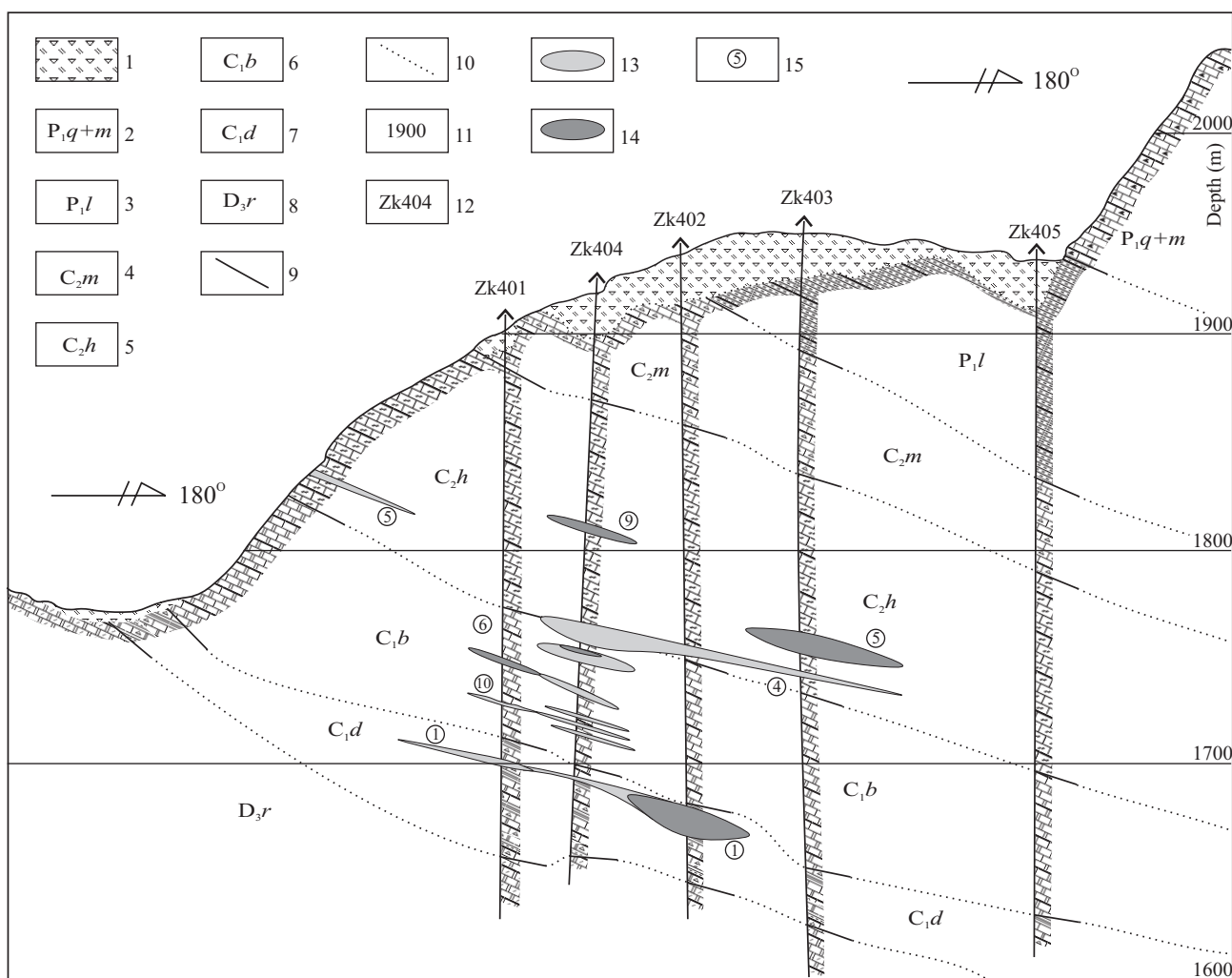


Fig. 3. The fourth prospecting line profile map of the Tianqiao Pb–Zn deposit.

1, Quaternary; 2, Qixia-Maokou Formation; 3, Liangshang Formation; 4, Maping Formation; 5, Huanglong Formation; 6, Baizuo Formation; 7, Datang Formation; 8, Rongxian Formation; 9, stratigraphic boundary; 10, rough estimate of stratigraphic boundary; 11, height mark; 12, drill hole and number; 13, oxidized ore; 14, primary sulfide ore; 15, ores and numbers.

Tianqiao Pb–Zn ore deposit are divided into the sedimentary epoch, hydrothermal epoch, and weathering epoch, of which the hydrothermal epoch could be divided into a further three ore-forming stages, that is, the pyrite–black sphalerite (Bl Sp)–calcite stage, the pyrite–brown sphalerite (Br Sp; brown–yellow, yellow–brown, and red–yellow, for short Br Sp)–galena–pyrite–calcite stage, and the light-yellow sphalerite (Ly Sp)–galena–calcite stage.

### 3 Samples and Analytical Methods

All the samples were collected from the main ore bodies and the different ore-forming stages. The samples were crushed by ore dressing to 40–60 mesh sizes. The individual minerals (sphalerites of different colors, galena, and pyrite) were then handpicked. All different-colored sphalerites were analyzed together with galena and pyrites. The analyses of the trace elements and REE were carried

out at Beijing Nuclear Industry Geology Academy, Beijing, China, using a high-resolution, inductively-coupled plasma mass spectrometer (ICP–MS; Finnigan MAT Co., Germany). This instrument has good precision, with  $2\sigma$  better than 10%, almost all the data are better than 5%. The analytical methods are as follows: (1) the samples were digested in 1 mL HF (hydrofluoric acid) and 2 mL HNO<sub>3</sub> (nitric acid) in a Teflon cup at 190°C for 40 h; (2) the cup was moved to the low-temperature, electric heating board; 1 mL HNO<sub>3</sub> was added and heated until the solution evaporated completely; (3) 500 ng Rh (1 mL) internal standard solution, 2 mL HNO<sub>3</sub>, and 3 mL deionized water were added to the Teflon cup accurately, and the cup was heated at 140°C for 5 h; and (4) 0.4 mL solution was transferred to a centrifuge tube, and 9.6 mL deionized water was added for the ICP–MS measurement. All acids and water were purified in an ultra-clean laboratory. The standard solutions were Ba600, OU-6, AMH-1, and GBPG

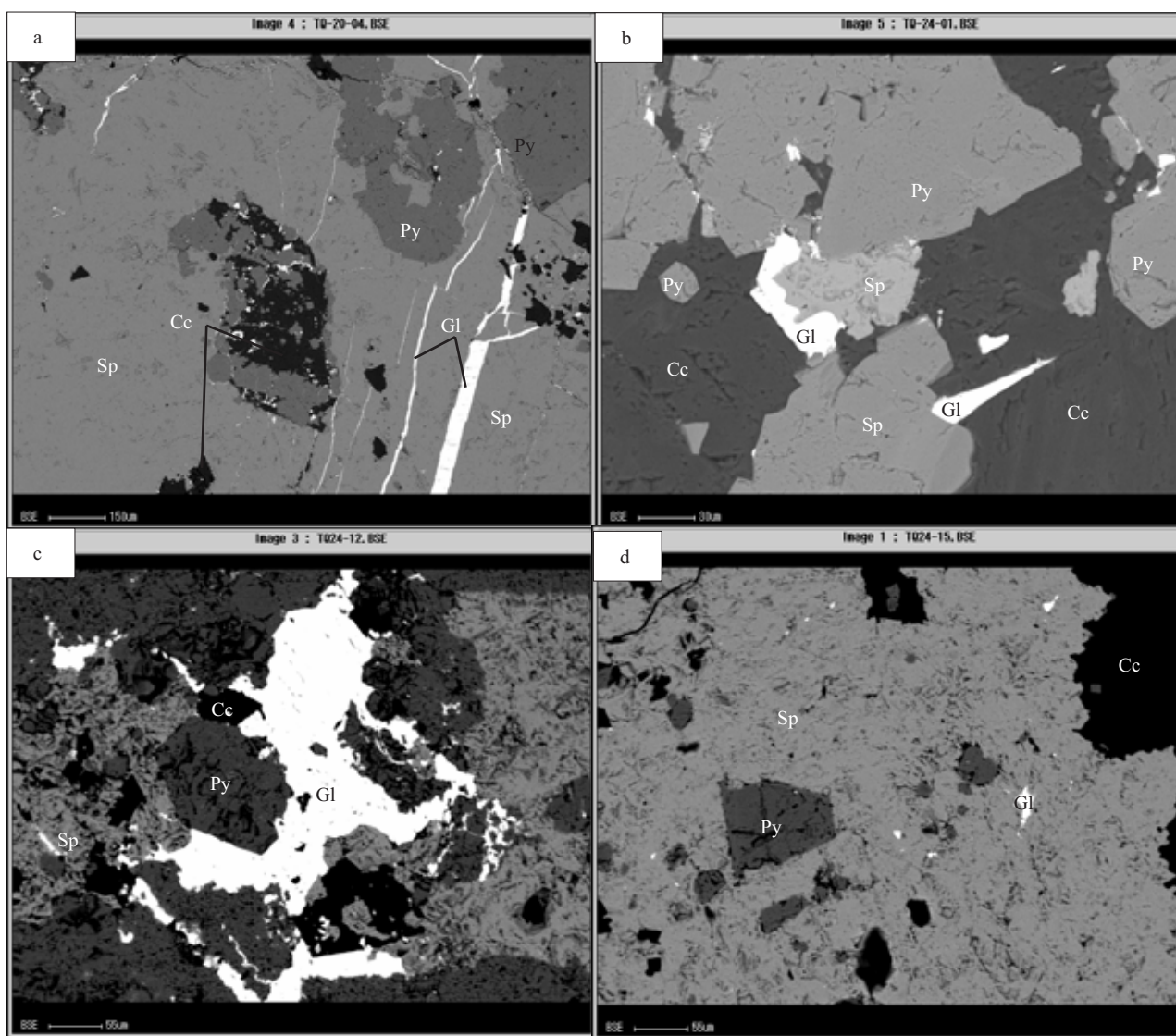


Fig. 4. Back-scattered electron images.

(a) Banded galena, and calcite and pyrite in sphalerite; (b) galena, pyrite, sphalerite, and calcite paragenesis; (c) replacement remnant sphalerite and galena; (d) automorphic pyrite and replacement remnant sphalerite.

-1. The testing errors of the standard solution were less than 5%. Detailed analytical methods are described in detail by Qi et al (2000).

## 4 Results

### 4.1 Trace elements in sulfides

The trace elements are listed in Table 1, from which we found that the trace element concentrations of Cu, Cd, Ga, Sn, As, and Sb are comparatively higher, especially the contents of Cd and Ga, which reached comprehensive utilization. Most of the useful elements were concentrated in sphalerite and galena, and the distribution characteristics are described. The trace elements V, Ni, Cu, As, Mo, Sn, Sb, Ga, Cd, In, and Se are concentrated in the sphalerites (Table 1). The mean V content in 13 sphalerites was 2.05

ppm, with a narrow range from 0.51 to 8.73 ppm. The mean Ni content in sphalerites was 2.25 ppm, with minimum and maximum contents of 0.67 and 3.62 ppm. The mean Cu content in sphalerites was 292.6 ppm, with a range from 69.8 to 501 ppm. The mean As content in sphalerites was 31.8 ppm, with minimum and maximum contents of 9.69 and 76.5 ppm. The mean Mo content in sphalerites was 6.52 ppm, with a wide range from 0.18 to 80.9 ppm. The mean Sn content in sphalerites was 89.1 ppm, with minimum and maximum contents of 16.2 and 247 ppm. The mean Sb content in sphalerites was 20.5 ppm, with a range from 3.71 to 59.3 ppm. The mean Ga content in sphalerites was 76.3 ppm, with minimum and maximum contents of 6.3 and 203 ppm. The mean Cd content in sphalerites was 771 ppm, with minimum and maximum contents of 623 and 938 ppm. The mean In content in the

sphalerite analyses was 3.96 ppm, with a range from 0.3 to 23.8 ppm. The mean Se content in sphalerites was 1.95 ppm, with a narrow range from 1.77 to 2.27 ppm.

For some trace elements (such as Ga and Cd) in sphalerites of different colors, the concentration contents in Ly Sp are higher than that in Br Sp and Bl Sp, and others (such as Ge, Tl, In, and Se) in Br Sp are higher than in Ly Sp and Bl Sp. However, in the different-colored sphalerites of the same sample (such as TQ24), the concentration regularity of Ge and In is Ly Sp > Br Sp > Bl Sp, and the Ga, Tl, Cd, and Se in Br Sp are higher than in Ly Sp and Bl Sp.

The trace elements Cu, As, Sn, Sb, Bi, Ge, Cd, and Tl are concentrated in galena. The mean Cu content in galenas was 25 ppm, with a range from 1.49 to 38.8 ppm. The mean As content in galena is 124.8 ppm, with minimum and maximum contents of 6.05 and 589 ppm. The mean Sn content in galena is 11 ppm, with minimum and maximum contents of 0 and 13.2 ppm. The mean Sb content in the galena analyses was 996 ppm, with a range from 275 to 1655 ppm. The mean Bi content in galena is 11.2 ppm, with minimum and maximum contents of 6.86–14.4 ppm. The mean Ge content in galena is 6.5 ppm, with minimum and maximum contents of 0 and 23.2 ppm. The mean Cd content in the galena analyses was 14.41 ppm, with a range from 3.62 to 40.6 ppm. The mean Tl content in the galena analyses was 6.3 ppm, with a range from 4.09 to 7.85 ppm.

In this study, only two of pyrites were separated from the Tianqiao Pb–Zn ore deposit. From the results, trace elements Cu and Sn were higher than other trace elements, with 57.5–75.9 ppm and 28.2–32.8 ppm, respectively. Almost all trace elements in pyrite are low, and are controlled by the crystal chemistry of pyrite (Liu et al., 1984) and the ore-forming environments (Zhou et al., 2009).

#### 4.2 REE in sulfides

The contents of REE in sulfide minerals from the Tianqiao Zn–Pb ore field are very low (Table 2). Total REE, excluding Y ( $\Sigma$ REE) of the two pyrite samples are 1.53 and 1.54 ppm, respectively.  $\Sigma$ REE are in the range of 0.11 to 2.27 ppm and 0.09 to 0.62 ppm in sphalerites and galenas, respectively. The contents of REE are highest in pyrite, moderate in sphalerite, and lowest in galena. This sequence in contents could be related to the gradual decrease in the strength of  $\text{Fe}^{2+}$ ,  $\text{Zn}^{2+}$ , and  $\text{Pb}^{2+}$  (Li et al., 2007). The same REE results could be obtained from the different samples (such as TQ19 and TQ60, Table 2).

In the sphalerite samples, the REE concentration regularity has the highest concentration in the Ly Sp, moderate in the Br Sp, and lowest in the Bl Sp, which is also shown in one sample (TQ24, Table 2). This sequence

**Table 1 Trace elements (ppm) contents and ratios of sulfide minerals of the Tianqiao Pb–Zn ore deposit**

No.	Object	Pyrite	Pyrite	TQ-19	TQ-3	TQ-25	TQ-24	TQ-24	TQ-25	TQ-16	TQ-54	TQ-10	TQ-24	TQ-24	TQ-24	TQ-19	TQ-3	TQ-13	TQ-60	TQ-26	TQ-18
				Pyrite	Galena	Galena	Galena	Galena	Ly Sp	Br Sp	Br Sp	Bl Sp	Ly Sp	Br Sp	Bl Sp	Br Sp	Bl Sp	Bl Sp	Ly Sp	Bl Sp	Bl Sp
V	0.75	1.05	—	—	—	—	—	—	0.79	8.73	1.77	2.79	1.1	1.81	1.43	1.52	2.16	0.78	0.51	2.11	1.12
Cr	0.84	0.54	—	—	—	—	—	—	—	—	0.031	1.11	0.77	2.08	0.28	0.15	—	0.034	—	1.23	1.09
Co	0.23	0.036	—	—	—	—	—	—	0.011	0.019	0.019	0.051	0.016	0.02	0.053	0.03	0.069	0.046	0.023	0.11	0.026
Ni	1.44	1.37	—	—	—	—	—	—	3.62	3.12	1.8	1.06	0.67	2.09	5.48	0.79	1.55	2.7	1.61	2.98	1.82
Cu	75.9	57.5	16.9	3.81	28.2	1.49	38.8	501	501	375	381	69.8	223	347	330	179	189	78	407	444	280
Zn	9811	3793	4798	1902	4776	157	19850	523236	16.2	30.1	39.5	14.5	9.69	25.8	65.2	11.9	34.8	12.4	576839	478288	485291
As	478	36.2	56.6	5.03	589	6.05	39.6	1.01	1.74	1.55	1.49	3.18	1.64	2.7	2.35	1.76	2.26	1.89	1.38	1.81	2.38
Sr	1.13	3.35	0.22	—	0.29	0.028	0.18	—	—	—	—	—	—	—	—	—	—	—	—	—	—
Zr	0.21	0.45	—	—	—	—	—	—	0.003	0.21	0.14	0.069	0.32	0.46	0.77	0.22	0.3	0.15	0.1	2.31	0.3
Nb	3.58	1.79	0.062	0.051	0.017	0.012	0.004	0.302	0.26	0.13	0.27	3.55	1.22	1.09	1.16	0.96	0.83	0.37	0.65	0.5	—
Mo	4.27	0.77	0.57	0.25	1.69	0.152	0.44	1.08	0.28	0.28	0.34	0.29	0.27	0.17	80.9	0.42	0.24	0.18	0.28	0.15	0.22
Sn	32.8	28.8	9.94	12.2	9.44	0.879	—	77.2	156	156	35.7	95.7	83.4	131	247	51.7	16.2	50.9	24.8	57.7	131
Sb	11.3	9.2	740	1399	1655	1049	1304	552	59.3	11.1	19.2	3.71	12.4	25.2	47.8	6.1	12.1	4.3	10.9	19.5	34.5
Ga	0.77	1.5	0.11	0.94	0.18	0.009	0.17	0.015	5.55	55.9	13.6	28.5	163	203	86.8	50.6	6.3	34.5	13	28.7	80.8
Ge	2.45	1.42	2.11	0.3	3.04	—	3.85	0.8	0.8	1.37	0.77	0.49	0.27	0.13	0.11	0.29	0.19	0.13	0.22	0.19	0.37
Cd	11.9	6.6	14.9	9.71	13.9	5.94	12.2	3.62	40.6	938	840	793	817	851	623	670	623	767	791	780	712
In	0.18	0.38	0.029	0.028	0.17	0.023	0.21	2.11	1.14	1.14	3.44	0.52	4.89	4.09	3.74	23.8	0.95	0.3	2.07	3.15	1.28
Re	0.007	0.002	0.001	0.001	0.004	0.002	0.005	0.003	0.003	0.003	0.002	0.006	0.002	0.002	0.006	0.002	0.001	0.003	0.003	0.001	0.005
Tl	0.46	0.29	6.9	5.91	4.09	6.72	7.85	4.9	0.32	0.51	0.19	1.87	0.37	0.33	0.57	0.15	0.33	0.34	0.14	0.28	3.91
Se	0.48	0.24	—	—	—	—	—	—	1.79	2.09	1.98	2.12	1.94	2.07	1.53	2.04	1.99	1.78	2.27	1.77	1.92
Co/Ni	0.16	0.03	—	—	—	—	—	—	—	—	—	—	—	—	—	—	—	—	—	—	—
Ga/In	—	—	—	—	—	—	—	—	108	49	4	55	33	50	23	2	7	115	6	9	63
Zn/Cd	824	575	322	196	384	100	391	489	558	652	643	590	671	662	704	796	771	609	729	613	682

Notes: Analysis conducted at the Beijing Nuclear Industry Geology Academy, greater than 5%; —, mean not detected. Bl Sp, black sphalerite; Br Sp, brown sphalerite; Ly Sp, light-yellow sphalerite.

in contents could be related to the gradual increase in the content of  $Zn^{2+}$  in sphalerites of different colors (Zhou et al., 2009).

Light rare earth element (LREE)/heavy rare earth element (HREE) ratios range from 0.52 to 12.45, except the ratios of galena (Table 2). Most of the sulfide samples have higher LREE/HREE ratios, which range from 1.12 to 12.45 (except one pyrite sample and two sphalerite samples), implying a strong REE fractionation between LREE and HREE, but the  $(La/Sm)_N$  and  $(Gd/Yb)_N$  values of pyrites and sphalerites are low (from 0.28 to 2.2 and from 0.25 to 3.92, respectively), suggesting that the inner fractionations of LREE and HREE are weak. On the chondrite-normalized REE patterns, the pattern curves of all sulfide samples showed flat type, with a significant Eu depletion.

The  $\delta Eu$  of all the sulfide samples range from 0.13 to 0.88 (except 1.3 of sample TQ16), which demonstrates a significant, negative anomaly. However, the Ce does not show a visible anomaly, with the values of  $\delta Ce$  ranging from 0.88 to 1.31.

## 5 Discussions

### 5.1 Ore-deposit genesis

In general, the trace elements in sphalerites, such as Ga, Cd, and In, contain much geologic information (Zhang, 1987; Palero-Fernández and Martín-Izard, 2005). The Ga/In ratio values of sphalerites in the Tianqiao Pb–Zn ore deposit are greater than 10 (Zhang, 1987), indicating that the deposit might be a strata-bound ore deposit. Tu et al. (1984) and Zhao et al. (2003) also analyzed the geologic setting and geochemistry of the SYG MA and concluded that it is a hydrothermal, strata-bound ore deposit; this result is in accordance with the results obtained in the present study. Zhang (1987) also used the  $\ln Ga-\ln In$  diagram to analyze the genesis of different Pb–Zn ore deposits. In the  $\ln Ga-\ln In$  diagram (Fig. 5), almost all of the samples fell into the sedimentary-reformed area, indicating that the Tianqiao Pb–Zn ore deposit might be sedimentary reformed. The Zn/Cd ratio values were more than 500, which also support this finding (Liu et al., 1984).

Zhang (1987) also studied the geology of trace elements in galena. In the  $\ln Bi-\ln Sb$  diagram (Fig. 6), almost all of the samples belonged to the sedimentary-reformed area. These results are similar to the results obtained earlier (Fig. 5).

Analyzing Co and Ni contents and the Co/Ni ratios in pyrite to determine the genesis of Pb–Zn ore deposits has proven to be useful (Hawley and Nichol, 1961; Price, 1972; Brill, 1989). Different pyrite generations have

Table 2 Rare earth elements (ppm) contents and parameters of sulfide minerals of the Tianqiao Pb–Zn ore deposit

No.	Object	TQ-60	TQ-19	TQ-3	TQ-25	TQ-46	TQ-54	TQ-24	TQ-24	TQ-24	TQ-10	TQ-24	TQ-24	TQ-19	TQ-3	TQ-13	TQ-60	TQ-26	TQ-18
		Pyrite	Pyrite	Galena	Galena	Galena	Galena	Galena	Ly Sp	Br Sp	Br Sp	Ly Sp	Br Sp	Br Sp	Br Sp	Br Sp	Ly Sp	Br Sp	Br Sp
La		0.051	0.152	0.064	0.076	0.078	0.046	0.099	0.041	0.019	0.025	0.068	0.08	0.13	0.058	0.13	0.021	0.16	0.033
Ce		0.146	0.465	0.069	0.02	0.02	0.005	0.17	0.074	0.012	0.064	0.217	0.163	0.258	0.147	0.242	0.055	0.32	0.984
Pr		0.027	0.059	0.01	0.003	0.003	0.003	0.02	0.01	0.003	0.012	0.032	0.024	0.032	0.02	0.023	0.012	0.005	0.112
Nd		0.184	0.283	0.064	0.024	0.02	0.023	0.146	0.057	0.022	0.066	0.189	0.112	0.133	0.108	0.125	0.082	0.03	0.424
Sm		0.116	0.087	0.029	0.064	0.064	0.041	0.085	0.027	0.025	0.038	0.123	0.05	0.042	0.042	0.038	0.037	0.015	0.036
Eu		0.005	0.006	0.006	0.006	0.006	0.006	0.014	0.003	0.006	0.007	0.007	0.005	0.005	0.005	0.006	0.002	0.002	0.006
Gd		0.126	0.072	0.006	0.006	0.006	0.006	0.034	0.017	0.008	0.018	0.12	0.042	0.033	0.035	0.03	0.029	0.013	0.025
Tb		0.03	0.017	0.005	0.004	0.006	0.006	0.007	0.004	0.002	0.003	0.031	0.011	0.009	0.01	0.008	0.008	0.004	0.004
Dy		0.216	0.097	0.005	0.006	0.006	0.006	0.024	0.023	0.016	0.026	0.198	0.07	0.066	0.069	0.045	0.051	0.018	0.029
Ho		0.041	0.017	0.003	0.003	0.003	0.003	0.003	0.004	0.008	0.005	0.041	0.016	0.014	0.014	0.009	0.009	0.004	0.008
Er		0.147	0.069	0.004	0.004	0.006	0.006	0.007	0.015	0.011	0.016	0.14	0.049	0.04	0.041	0.034	0.026	0.013	0.023
Tm		0.041	0.018	0.003	0.003	0.003	0.003	0.003	0.003	0.003	0.004	0.04	0.012	0.012	0.011	0.009	0.008	0.006	0.005
Yb		0.353	0.158	0.005	0.008	0.006	0.005	0.007	0.028	0.026	0.024	0.329	0.106	0.105	0.111	0.081	0.076	0.03	0.051
Lu		0.061	0.027	0.003	0.003	0.003	0.003	0.003	0.006	0.004	0.006	0.056	0.019	0.018	0.016	0.015	0.011	0.005	0.007
ΣREE		1.54	1.53	0.25	0.20	0.21	0.12	0.62	0.31	0.19	0.11	1.59	0.76	0.89	0.8	0.43	0.19	2.27	0.45
LREE		0.53	1.05	0.24	0.18	0.19	0.12	0.53	0.21	0.11	0.07	0.64	0.43	0.6	0.38	0.57	0.21	1.1	2.1
HREE		1.02	0.48	0.01	0.02	0.02	0.01	0.08	0.1	0.08	0.04	0.96	0.33	0.29	0.31	0.23	0.09	0.17	0.15
LREE/HREE		0.52	2.21	0.02	0.02	0.02	0.01	6.51	2.12	1.37	2.08	0.67	1.34	2.03	1.24	2.45	0.97	1.12	12.45
δEu		0.13	0.23	0.003	0.003	0.003	0.003	0.8	0.43	1.3	0.88	0.18	0.33	0.41	0.4	0.54	0.47	0.44	0.68
δCe		0.95	1.18	0.003	0.003	0.003	0.003	0.92	0.88	1.02	0.89	1.12	0.9	0.97	1.04	1.05	0.83	0.86	0.96
$(La/Sm)_N$		0.11	0.65	0.63	6.4	8.76	6.2	9.54	0.99	0.49	0.74	0.7	0.14	0.51	0.86	1.11	0.19	0.36	7.14
$(La/Sm)_N$		0.28	1.1	1.39	0.75	0.77	0.71	3.92	0.96	0.48	0.41	0.35	1.01	1.82	2.2	0.36	0.67	9.44	0.58
$(Gd/Yb)_N$		0.29	0.37	0.003	0.003	0.003	0.003	3.92	0.49	0.25	0.61	0.29	0.32	0.25	0.3	0.31	0.35	0.57	0.39

Notes: Analysis conducted at the Beijing Nuclear Industry Geology Academy, greater than 5%; –, mean not detected. Bl Sp, black sphalerite; Br Sp, brown sphalerite; Ly Sp, light-yellow sphalerite.

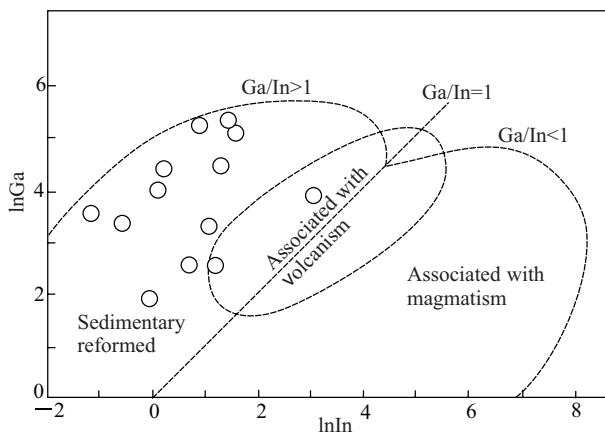


Fig. 5. InGa vs. lnIn of sphalerite (after Zhang, 1987).

different Co/Ni values; the Co/Ni values associated with volcanism, sedimentary-reformed and hydrothermal genesis ore deposits are  $>5-10$ ,  $<1$ , and  $<5$ , respectively (Price, 1972). The  $<0.5$  Co/Ni value of pyrite in the Tianqiao Pb–Zn ore deposit indicates that it could belong to a sedimentary-reformed area, which is in accordance with the above-mentioned results.

The ratios of Ga/In, Zn/Cd, and Co/Ni of the Tianqiao Pb–Zn ore deposit are different from the ratios of the Volcanogenic Massive Sulfide-type (VMS) and Sedimentary Exhalative-type (SEDEX) Pb–Zn ore deposits (Zhang, 1987; Huang et al., 2004; Palero-Fernández and Martín-Izard, 2005; Li et al., 2007), but are close to the ratios of the Mississippi valley-type (MVT) Pb–Zn ore deposits. Many researchers have considered the deposit model to be MVT (Zhou et al., 2001; Jin, 2008). However, the result conflicts with the geologic–tectonic setting and geochemical evidence (Huang et al., 2004; Zhou et al., 2009).

The Tianqiao Pb–Zn ore deposit was situated in the central Yadu–Ziyun discordogenic fault zone (Fig. 1), which was formed at the end of the Late Ordovician Duyun Movement (Jin, 2008). It was an important magmatic channel of Emeishan basalts (Liu, 2002; Jin et al., 2007). The ore bodies were controlled by the  $F_{37}$  fault, which shows a stratoid shape, platy ore body, and lenticular form (Figs. 2, 3). The geologic and tectonic characteristics indicate that the deposit was an epigenetic deposit (Jin, 2008; Zhou et al., 2009). The S, C, O, and Pb isotopic data also show that the sulfurs in the ore-forming fluids should be derived from the thermochemical sulfate reduction of marine sulfates from the sedimentary stratum;  $\text{CO}_2$  might have come from marine carbonate dissolution, and Pb had crust-derived features (Huang et al., 2004; Jin, 2008; Zhou et al., 2010). Therefore, the deposit was sedimentary genesis, and was reformed by hydrothermal solutions. The ratios of Ga/In and Zn/Cd in sphalerites, the lnGa–lnIn diagram of sphalerites, and the lnBi–lnSb diagram of

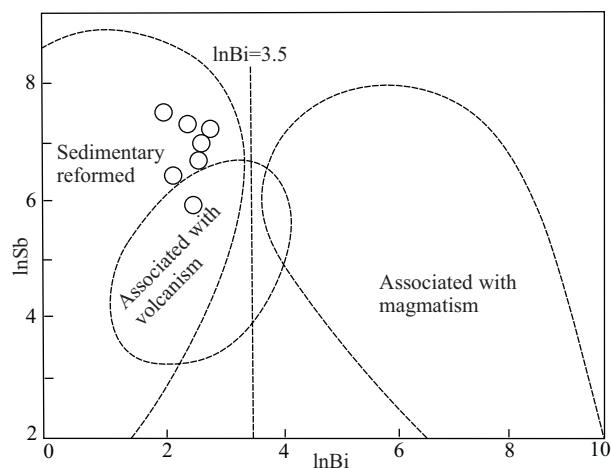


Fig. 6. lnBi vs. lnSb of galena (after Zhang, 1987).

galenas, together with the Co/Ni ratios of pyrites, indicate that the genesis of the Tianqiao Pb–Zn ore deposit could be a hydrothermal, sedimentary-reformed type.

## 5.2 Origin of ore-forming materials/fluids

REE are very useful in analyses of the origin of ore-forming fluids and metals (Barrett et al., 1990; Bau, 1991; Mills and Elderfield, 1995; Wilkinson et al., 2005). They have similar chemical properties and behave coherently in most geochemical processes (Wang et al., 1989). However, according to coordination chemistry (Dai, 1987),  $\text{REE}^{3+}$  and  $\text{Ce}^{4+}$  are hard acids, whereas  $\text{Eu}^{2+}$  is a soft acid (Chen and Fu, 1991; Chen and Zhao, 1997; Ma and Liu, 1999). Thus, it is easy for  $\text{Eu}^{2+}$  to separate from the other  $\text{REE}^{3+}$  ions during the geochemical process, resulting in negative or positive Eu anomalies on chondrite-normalized REE patterns for geologic samples (Li et al., 2007). In the process of water–rock reaction, the solid products in a reducing environment have a high  $\delta\text{Eu}$  value (usually  $>1$ ), low  $\Sigma\text{REE}$  values, and high LREE/HREE ratios; in contrast, the oxidizing conditions show low  $\delta\text{Eu}$  values (usually  $<1$ ), high  $\Sigma\text{REE}$  values, and low LREE/HREE ratios (Chen and Fu, 1991; Chen and Zhao, 1997; Ma and Liu, 1999). The above-mentioned process is called the redox model for REE geochemical evolution (Chen and Fu, 1991).

The sphalerites and pyrites of the Tianqiao Pb–Zn ore deposit have low  $\Sigma\text{REE}$  values ( $<3$  ppm) and high LREE/HREE ratios (1.12–12.45); the Eu shows negative anomaly, and Ce shows weakly-positive anomaly (Table 2; Fig. 7a). The REE of the same sample (TQ24, TQ19, and TQ60) of different-colored sphalerites (Fig. 7b) and different minerals (Fig. 7c), and the REE of ore, pyrite, calcite, and sphalerite (Fig. 7d) show the same result. This conclusion is supported by the mineral association that is rich in sulfides, formed by a fluid system with high activity of  $\text{S}^{2-}$ . The high  $\text{S}^{2-}$  activity is an indubitable indicator of a reducing



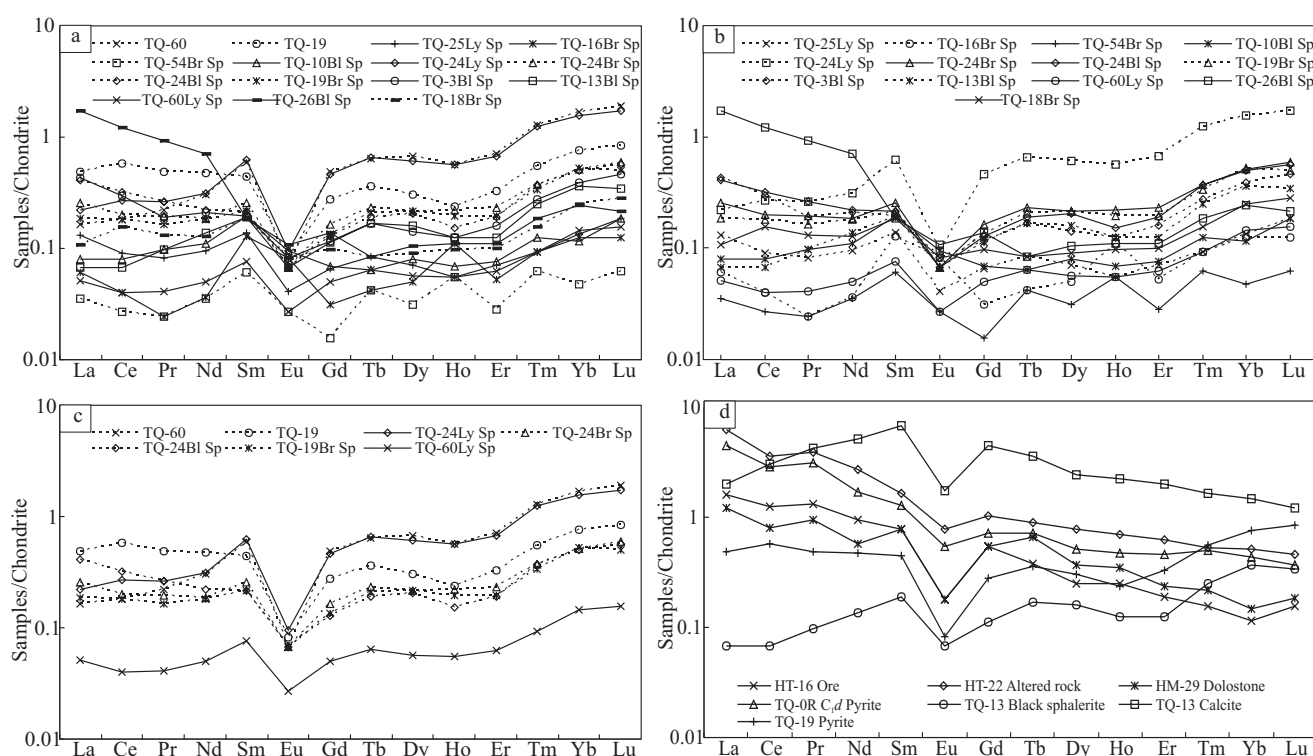


Fig. 7. Chondrite-normalized rare earth element (REE) patterns (after Boynton, 1984).

(a) Chondrite-normalized REE patterns of different minerals; (b) Chondrite-normalized REE patterns of different-colored sphalerites; (c) Chondrite-normalized REE patterns of pyrite and sphalerite in samples of TQ19, TQ24, and TQ60; (d) Chondrite-normalized REE patterns of different samples (HT-16 ore is an ore sample; HT-22 altered rock is an altered wall-rock sample; HM-29 dolostone is a stratum dolostone sample; TQ-0RC Datang Formation ( $C_1d$ ) pyrite is a pyrite sample from  $C_1d$  stratum (data com from Mao, 2001). TQ-13 calcite is a calcite sample (unpublished data). All figures are drawing in logarithmic coordinates.

environment. According to the redox model for REE geochemical evolution, the sulfides from the Tianqiao ore deposit, which were formed in reducing conditions, should have high Eu values instead of Eu depletion (Table 1). This can be interpreted by considering the following two possibilities: (1) the fluid system and its source might be depleted in Eu; and (2) calcite, the gangue mineral coexisting with sulfides, is enriched in Eu, resulting in Eu-depleted sulfides to maintain the Eu mass balance. Calcite is almost the only gangue mineral in the Tianqiao ore deposit, and other gangue minerals are rare. The calcites show negative Eu anomalies (Fig. 7). This rules out the second possibility/hypothesis that the coexisting calcite was enriched in Eu, while sulfides were depleted in Eu to maintain the Eu mass balance.

Many researchers believed that the wall rocks were the main sources, while other researchers believed that the ore-forming fluids and metals were from the ore-bearing wall rocks themselves (Chen, 1986), the stratum below, the crystalline basement (Zheng, 1994; Qian, 2001), and the Emeishan basalt (Huang et al., 2004). Huang et al., (2004) and Jin (2008) proved that the chondrite-normalized REE patterns, with Eu-depleted characters of different chronostratigraphic units, were the same as the REE of sulfide minerals. This finding is in accordance with the first

possibility/hypothesis, that is, the fluid systems and their sources might be depleted in Eu. This means that the main sources of the Tianqiao Pb–Zn ore deposit are the from different chronostratigraphic units.

From the above-mentioned discussion, we can conclude that the ore-forming fluids/metals could be from the polycomponent systems, and this finding is in accordance with that of Huang et al. (2004).

## 6 Conclusions

The trace elements of sulfide minerals from the Tianqiao Pb–Zn ore deposit are important for mineralogy and comprehensive utilization. It was concluded that in the Tianqiao Pb–Zn ore field, the trace elements V, Cu, Sn, Ga, Cd, In, and Se are concentrated in sphalerite; the Sb, As, Ge, and Tl are concentrated in galena; and almost all of the trace elements in pyrite are low. At the same time, the ratios of Ga/In and Zn/Cd, the  $\ln\text{Ga}–\ln\text{In}$  diagram of sphalerites, and the  $\ln\text{Bi}–\ln\text{Sb}$  diagram of galena, together with the Co/Ni ratios of pyrite, indicate that the genesis of the Tianqiao Pb–Zn ore deposit could be hydrothermal, sedimentary reformed-type.

Sulfide minerals of the Tianqiao Pb–Zn ore deposit have very low REE contents, high LREE/HREE ratios, and

negative Eu anomalies. These sulfides were deposited in a reducing environment from Eu-depleted fluid systems. The REE geochemical characteristics of the sulfides are similar to those of carbonate host rocks, which indicate that the ore-forming fluids could be from the carbonate host rocks, underlying strata, and basement rocks.

## Acknowledgements

This research was supported by the National Basic Research Program of China (grant no. 2007CB411402). The authors thank Professor Zhang Hui (Institute of Geochemistry, Chinese Academy of Sciences), Professor Li Wenbo and Xu Cheng (Peking University) for their insightful suggestions. Thanks are also due to Dr Hou Weiguo (Institute of Geochemistry, Chinese Academy of Sciences) for his help in improving the quality of the manuscript.

Manuscript received Oct. 19, 2009  
accepted March 15, 2010  
edited by Jiang Shaoqing

## References

- Bau, M., 1991. Rare-earth element mobility during hydrothermal and metamorphic fluid-rock interaction and the significance of the oxidation state of europium. *Chemical Geology*, 93(3–4): 219–230.
- Barrett, T.J., Jarvis, I.J., and Kym, E., 1990. Rare earth element geochemistry of massive sulfides-sulfates and gossans on the Southern Explorer Ridge. *Economical Geology*, 18: 583–586.
- Brill, B.A., 1989. Trace-element contents and partitioning of elements in ore minerals from the CSA Cu-Pb-Zn Deposit, Australia, and implications for ore genesis. *Canadian Mineralogist*, 27(2): 263–274.
- Chen Yanjing and Fu Shigu, 1991. Variation of REE patterns in early Precambrian sediments: Theoretical study and evidence from the southern margin of the northern China craton. *Chinese Sci. Bull.*, 36 (13): 1100–1104.
- Chen Yanjing and Zhao Yongchao, 1997. Geochemical characteristics and evolution of REE in the Early Precambrian sediments: Evidences from the southern margin of the North China craton. *Episodes*, 20: 109–116.
- Chen Shijie, 1986. A discussion on the origin of Pb-Zn deposits in western Guizhou and northeastern Yunnan. *Guizhou Geology*, 3(3): 211–222 (in Chinese with English abstract).
- Dai Anbang, 1987. Coordination Chemistry. *Beijing: Science Press*, 750 (in Chinese).
- Gu Shangyi, 2006. Characteristics of REE composition within Pb-Zn deposits in northwestern Guizhou: in addition to a discussion of relationship between Pb-Zn deposits and Emeishan basalts in northwestern Guizhou. *Guizhou Geology*, 23(4): 274–277 (in Chinese with English abstract).
- Guang Shiping and Li Zhongxiong, 1999. Lead-Sulfur isotope study of carbonate-hosted Pb-Zn deposits at the eastern margin of the Kangdian axis. *Geology Geochemistry*, 27(4): 45–54 (in Chinese with English abstract).
- Hawley, J.E., and Nichol, I., 1961. Trace elements in pyrite, pyrrhotite and chalcopyrite of different ores. *Economic Geology*, 56(3): 467–487.
- Han Runsheng, Liu Congqiang, Chen Jin, Ma Deyun and Li Yuan, 2001. Study on the metallogenic model of the Huize Pb-Zn deposit in Yunnan Province. *Acta Mineralogica Sinica*, 21: 674–680 (in Chinese with English abstract).
- Han Runsheng, Liu Congqiang, Huang Zhilong, Ma Deyun, Li Ying, Hu Bing, Ma Gesheng and Lei Li, 2004. Fluid inclusions of calcite and sources of ore-forming fluids in the Huize Zn-Pb-(Ag-Ge) district, Yunnan Province, China. *Acta Geologica Sinica* (English edition), 78: 583–591.
- Huang Zhilong, Chen Jin, Han Runsheng, Li Wenbo, Liu Congqiang, Zhang Zhenliang, Ma Deyun, Gao Derong and Yang Hailin, 2004. *Geochemistry and ore-formation of the Huize giant lead-zinc deposit, Yunnan, Province, China: discussion on the relationship between Emeishan Flood basalts and lead-zinc mineralization*. Beijing: Geological Publishing House (in Chinese).
- Huang Zhilong, Li Xiaobiao, Zhou Meifu, Li Wenbo and Jin Zhongguo, 2010. REE and C-O Isotopic Geochemistry of Calcites from the World-class Huize Pb-Zn Deposits, Yunnan, China: Implications for the Ore Genesis. *Acta Geologica Sinica* (English edition), 84(3): 597–613.
- Huang Zhilong, Xu Cheng, Andrew McCAIG, Liu Congqiang, Wu Jing, Xu Deru, Li Wenbo, Guan Tao and Xiao Huayun, 2007. REE geochemistry of fluorite from the Maoniuping REE deposit, Sichuan Province, China: Implications for the source of ore-forming fluids. *Acta Geologica Sinica* (English edition), 81(4): 622–636.
- Jin Zhongguo, Zhang Lunwei and Ye Jing, 2007. Ore-forming materials source of lead-zinc deposit in the northwest Guihou. *Geology and Prospecting*, 43(6): 32–35 (in Chinese with English abstract).
- Jin Zhongguo, 2008. *The ore-control factors, ore-forming regularity and forecasting of Pb-Zn deposit, in northwestern Guizhou Province*. Beijing: Engine Industry Press, 1–105 (in Chinese).
- Kamona, A.F., and Friedrich, G.H., 2007. Geology, Mineralogy and stable isotope geochemistry of the Kabwe carbonate-hosted Pb-Zn deposit, Central Zambia. *Ore Geology Reviews*, 30: 217–243.
- Li Wenbo, 2004. *The geochemistry and ages of the Huize Zn-Pb ore field, Yunnan Province*. Doctor's degree dissertation Guiyang: Institute of Geochemistry, CAS.1–100 (in Chinese with English abstract).
- Li Wenbo, Huang Zhilong, Chen Jin, Han Runsheng, Guan Tao, Xu Cheng, Gao Derong and Zhao Deshun, 2002. Sources of ore-forming materials of the giant Huize zinc-lead deposit, Yunnan Province: Evidence from contents of ore-forming elements in the wall rocks and Emeishan basalt in this district. *Mineral Deposits* (supp1), 21: 413–416 (in Chinese with English abstract).
- Li Wenbo, Huang Zhilong and Qi Liang, 2007. REE geochemistry of sulfides from the Huize Zn-Pb ore field, Yunnan Province: Implication for the sources of ore-forming metals. *Acta Geologica Sinica* (English edition), 81(3): 442–449.
- Liao Wen, 1984. Mineralization model and the characters of isotope composition of S and Pb in the Pb-Zn metallic area in the East and West Yunnan Province, China. *Geology and Prospecting*, 1: 1–6 (in Chinese with English abstract).

- Liu Hechang and Lin Wenda, 1999. *Study on the Law of Pb-Zn-Ag ore deposits in Northeast Yunnan, China*. Kunming: Yunnan University Press, 389 (in Chinese).
- Liu Yingjun, Cao Liming, Li Zhaolin, et al., 1984. *Elements geochemistry*. Beijing: Science Press, (in Chinese).
- Liu Youping, 2002. Preliminary study on the metallogenic regulation and the prospecting model for the Pb-Zn deposits in the areas of northwest Guizhou. *Guizhou Geology*, 19(3): 169–174 (in Chinese with English abstract).
- Ma Yingjun and Liu Congqiang, 1999. Trace element geochemistry during weathering as exemplified by the weathered crust of granite, Longnan, Jiangxi. *Chinese. Sci. Bull.*, 44: 2260–2263.
- Mao Deming, 2001. REE geochemistry of Pb-Zn deposits in northwestern Guizhou and Its significance. *Guizhou Geology*, 18(1): 12–17 (in Chinese with English abstract).
- Mills, R.A., and Elderfield, H., 1995. Rare earth element geochemistry of hydrothermal deposits from the active TAG Mound, 26° N Mid-Atlantic Ridge. *Geochimica et Cosmochimica Acta*, 59(17): 3511–3524.
- Palero-Fernández, F.J., and Martín-Izard, A., 2005. Trace element contents in galena and sphalerite from ore deposits of the Alcudia Valley mineral field (Eastern Sierra Morena, Spain). *Journal of geochemical exploration*, 86: 1–25.
- Price, B.J., 1972. *Minor Elements in Pyrites from the Smithers Map Area, British Columbia and Exploration Applications of Minor Element Studies (Doctoral dissertation)*. Vancouver: Columbia University.
- Qi Liang, Hu Jing and Gregoire D.C., 2000. Determination of trace elements in granites by inductively coupled plasma mass spectrometry. *Talanta*, 51: 507–513
- Qian Jianping, 2001. Tectonic-dynamic mineralization in Weining-Shuicheng Pb-Zn ore belt, northwestern Guizhou. *Geology-Geochemistry*, 29(3): 134–139 (in Chinese with English abstract).
- Tu Guangchi, Gao Zhenmin, Hu Ruizhong, Zhang Qian, Li Chaoyang, Zhao Zhenhua and Zhang Baogui, 2003. *Geochemistry and mineralization of the dispersed elements*. Beijing: Science Press, 1–407 (in Chinese).
- Tu Guangchi, 1984. *The geochemistry of stratabound deposit, China*. Beijing: Geology Press, 13–54 (in Chinese).
- Wang Linjiang, 1994. Geological and geochemical features of lead-zinc deposits in northwestern Guizhou. *Journal of Guilin College of Geology*, 14(2): 125–130 (in Chinese with English abstract).
- Wang Yuwang, Wang Jingbin, Wang Lijuan, Wang Yong and Tu Caineng, 2004. REE Characteristics of the Kalatongke Cu-Ni Deposit, Xinjiang, China. *Acta Geologica Sinica* (English edition), 78(2): 396–403.
- Wang Zhonggang, Yu Xueyuan and Zhao Zhenhua, 1989. *Geochemistry of Rare Earth Elements*. Beijing: Science Press, 535 (in Chinese).
- Wilkinson, J.J., Eyre, S.L., and Boyce, A.J., 2005. Ore-forming processes in Irish-type carbonate-hosted Zn-Pb deposits: evidence from mineralogy, chemistry, and isotopic composition of sulfides at the Lisheen Mine. *Economic Geology*, 100: 63–86.
- Zhang Qian, 1987. Trace elements in galena and sphalerite and their geochemical significance in distinguishing the genetic types of Pb-Zn ore deposits. *China. J. Geochem.*, 6(2): 177–130.
- Zhang Yunxiang, Luo Yaonan and Yang Congxi, 1988. *Panzhuhua- Xichang Rift in China*. Beijing: Geological Publishing House, 290–297 (in Chinese).
- Zhao Zhenhua, Tu Guangchi, et al., 2003. *The super-large deposits, China* (II). Beijing: Science Press, 1–617 (in Chinese).
- Zheng Chuanlun, 1992. Study on ore-controlling structures of Pb-Zn ore region in northwestern Guizhou Province. *Mineral Resources and Geology*, 6(3): 193–200 (in Chinese with English abstract).
- Zheng Chuanlun, 1994. An approach on the source of ore-forming metals of Pb-Zn deposits in northwestern Guizhou Province. *Journal of Guilin College of Geology*, 14(2): 113–124 (in Chinese with English abstract).
- Zhou Chaoxian, Wei Chunsheng, Guo Jiyun and Li Chaoyang, 2001. The source of metals in the Qilinchang Zn-Pb deposit, Northeastern Yunnan, China: Pb-Sr isotope constraints. *Economic Geology*, 96: 583–598.
- Zhou Jiayi, Huang Zhilong, Li Xiaobiao, Zhou Guofu, Liu Shirong, Fu Shaohong and Zheng Wenqin, 2008. The new evidence about the germanium concentrates in the galena of Huidong Daliangzi large-scale Pb-Zn deposit, Sichuan Province, China. *Acta Mineralogica Sinica*, 28(4): 473–475 (in Chinese with English abstract).
- Zhou Jiayi, Huang Zhilong, Zhou Guofu, Li Xiaobiao, Ding Wei and Gu Jing, 2009. The occurrence state and regularity of dispersed elements in Tianqiao Pb-Zn ore deposit, Guizhou Province, China. *Acta Mineralogica Sinica*, 29(4): 471–480 (in Chinese with English abstract).
- Zhou Jiayi, Huang Zhilong, Zhou Guofu, Li Xiaobiao, Ding Wei and Bao Guangping, 2010. Sulfur isotopic compositions of the Tianqiao Pb-Zn ore deposit, Guizhou Province, China: implications for the source of sulfur in the ore-forming fluids. *China. J. Geochem.*, 29(3): 301–306.